The Full Phase Behavior for Block Copolymers in Solvents of Varying Selectivity

Timothy P. Lodge,*,† Bryant Pudil,‡ and Kenneth J. Hanley§

Department of Chemistry and Department of Chemical Engineering & Materials Science, University of Minnesota, Minneapolis, Minnesota 55455-0431

Received January 22, 2002

ABSTRACT: The phase behavior of six poly(styrene-*b*-isoprene) (SI) diblock copolymers has been mapped out in the styrene-selective solvents di-*n*-butyl phthalate (DBP), diethyl phthalate (DEP), and dimethyl phthalate (DMP). The polymer molecular weights were chosen to make the melt order−disorder transition (ODT) experimentally accessible, and the styrene compositions f ranged from 0.23 to 0.70, to access the full range of melt morphologies. For each polymer a phase diagram was constructed, with polymer volume fractions, ϕ, ranging from 0.01 to 1.0 and temperatures, T, from 0 to 250 °C. Phase assignments were based on small-angle X-ray scattering (SAXS), and the ODTs and order−order transitions (OOTs) were located by a combination of SAXS, rheology, and static birefringence. The critical micelle temperatures (cmt) in dilute solution were determined by dynamic light scattering. In this manner the full "phase cube" was mapped out in each solvent, enabling generation of phase maps (ϕ,f) at constant T and (f,T) at constant ϕ. The solvents range from slightly to strongly selective, in the sequence DBP, DEP, and DMP, and in each case the selectivity diminishes with increasing T. This property gives rise to a plethora of thermally induced OOTs, and several solutions exhibit four distinct equilibrium phases upon heating. In addition to the eight phases well established for SI copolymers in the melt (a body-centered-cubic (bcc) array spheres of styrene or isoprene, hexagonally packed cylinders of styrene or isoprene, gyroid with isoprene or styrene matrix, lamellae, disordered), broad regions of lamellae + cylinder coexistence and face-centered-cubic (fcc) isoprene spheres were observed. The sequence of phases could be broadly understood in terms of changes in spontaneous interfacial curvature arising from differential swelling of the two microdomains. For a given polymer and solvent, the ODT varied smoothly with ϕ from the melt value down toward the dilute solution critical micelle temperature (cmt); at about $\phi \approx 0.2$ the ordered phases gave way to a solution of micelles. In some cases solutions near $\phi \approx 0.2$ exhibit reentrant ODTs, as they evolved from a solution of micelles to an fcc (and/or bcc) lattice, to a solution of chains, upon heating. The origins of these various phenomena are discussed, and the results are compared and contrasted with other measurements on SI copolymers in the literature.

Introduction

The addition of a selective solvent to a block copolymer can greatly expand the range of accessible self-assembled morphologies.[1−9] In this case "selective" denotes the thermodynamic preference of the diluent for one of the two blocks. In the strongly selective limit, the solvent will partition almost entirely into one microdomain; a common example is water mixed with nonionic surfactants (e.g., hydrocarbon/ethylene oxide diblocks).[10,11] In the other limit, the solvent is said to be "neutral", and the solvent exhibits no preferential partitioning; toluene and dioctyl phthalate mixed with styrene−isoprene copolymers are two examples of this case.[12,13] The selectivity may also be a significant function of temperature. For example, if there is an accessible Θ temperature for the solvent and the less preferred block, the solvent may approach neutrality once the Θ temperature is exceeded but be quite strongly selective well below the Θ point. For a given polymer/solvent system, the phase behavior may be represented by a cube as shown in Figure 1. The rear face represents the melt phase map, plotted as temperature, T, vs the copolymer composition, f. In mean-field theory, T is inversely related to the degree of segregation, χN, where N is the degree of polymerization and χ is the Flory−Huggins interaction parameter between the segments of the two blocks. The remaining axis is the polymer volume fraction in solution, ϕ. For a given copolymer (f,N) a phase diagram may be constructed in the (ϕ,T) plane. Once this has been accomplished for several polymers of different f, phase maps in the two other planes can be determined, i.e., (f,ϕ) at constant T and (f,T) at constant ϕ.

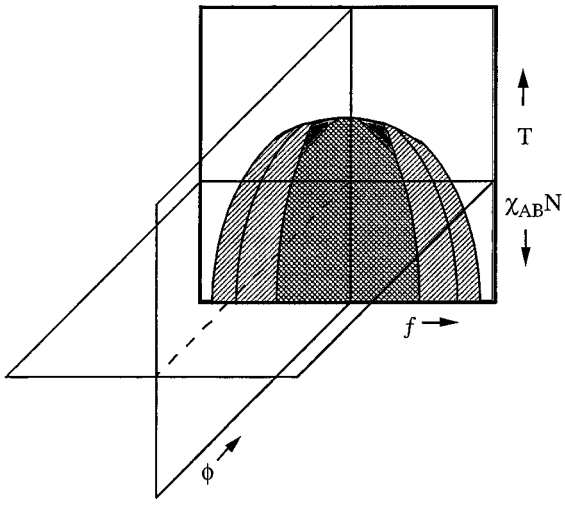

Figure 1. Schematic illustration of the block copolymer solution phase cube, as a function of temperature, T, copolymer composition, f, and copolymer concentration, ϕ. The shaded plane corresponds to the melt phase map.

* Author for correspondence: e-mail lodge@chem.umn.edu.
† Department of Chemistry.
‡ Current address: Polymerix Corporation, Voorhees, NJ 08043.
§ Current address: 3M Company, St. Paul, MN 55144.

10.1021/ma0200975 CCC: $22.00
Published on Web 05/10/2002

In this report we describe the phase behavior of six poly(styrene-*b*-isoprene) (SI) diblock copolymers mixed with three different solvents: di-*n*-butyl phthalate (DBP), diethyl phthalate (DEP), and dimethyl phthalate (DMP). The accessible temperature range extends from 0 up to 250 °C, a remarkably wide interval made possible by the low volatility and glass-forming nature of the solvents. The concentrations range from the bulk ($\phi = 1$) down to the dilute limit ($\phi = 0.01$). The copolymer compositions (styrene volume fractions) range from 0.23 to 0.70, and the molecular weights are chosen to make the bulk order−disorder transition temperatures (ODT) accessible or nearly so. All three solvents favor the polystyrene block, but to differing degrees; DBP is slightly selective, DEP is more selective, and DMP is strongly selective. In a separate report, we describe the phase behavior of the same copolymers in the neutral solvent DOP,[14] and in another we have examined the behavior of one of these copolymers in DBP and DEP.[8] Thus, the current results, in combination with the other reports, provide a thorough compendium of block copolymer solution phase behavior.

This study is related in some aspects to previous documentation of binary surfactant/solvent phase behavior. For example, the systems poly(ethylene oxide-*b*-propylene oxide) (PEO−PPO) and poly(ethylene oxide-*b*-butylene oxide) (PEO−PBO) in water have received much attention.[1,15−20] These systems share the rich morphological polymorphism displayed by the organic analogues, and the sequence of ordered phases upon changing ϕ or T is often similar, but there are differences. First, much of the PEO−PPO work has involved ABA triblock copolymers, which is a modest perturbation when PEO is the A block but not when it is the B block. Second, the solvent quality of water decreases with increasing T, so that some of the thermotropic order−order transitions and ODTs are inverse to those described here. Third, these systems display an intermediate structure often referred to as "soft gel", which apparently has no analogue in the organic solvent case; the so-called "hard gel" in these systems is simply an ordered cubic phase. Fourth, and most importantly in this context, water tends to be strongly selective. Although some degree of variation in selectivity may be accomplished by changing the unfavorable block, there is no aqueous analogue to the progression that the series DOP, DBP, DEP, and DMP affords. Similarly, low molecular weight ionic surfactants in water show very rich phase behavior, but solvent selectivity is not an experimentally accessible variable.

Aspects of the phase behavior of SI and other diblock copolymers in selective organic solvents have been considered previously by several groups.[1−3,6,9] Early work was reviewed by Sadron and Gallot; the strong similarity between the effects of adding selective solvent and the effect of changing composition in the bulk was emphasized.[2] More recent results that bear direct comparison with ours are those of McConnell and Gast[6] and Lai et al.[9] McConnell and Gast employed various SI diblocks in the isoprene-selective solvent, decane, as a function of concentration at fixed temperature.[6] Our results contradict theirs in certain respects, for reasons we will consider in the Discussion section. Lai et al. employed SI diblocks in the isoprene-selective solvent tetradecane, and also to some extent in the more selective squalane and tributylamine, and conducted phase behavior studies over a wide range of concentration and temperature.[9] In the main our results are complementary to theirs, in that we emphasize styrene-selective solvents, and the overall phenomenology is very similar. However, there are significant differences that may be attributed primarily to the stronger temperature dependence of the solvent selectivity in the case of the dialkyl phthalates.

Table 1. Sample Characteristics

sample	M_{PS}	M_{PI}	M_w/M_n	N	f_{PS}
SI(11−32)	$10._9$	$31._6$	1.02	456	0.23
SI(11−21)	$10._7$	$20._7$	1.05	333	0.31
SI(15−13)	$14._8$	$12._8$	1.02	285	0.50
SI(8−7)	$8._0$	$7._0$	1.01	155	0.49
SI(22−12)	$21._9$	$12._4$	1.03	348	0.61
SI(38−14)	$37._8$	$14._4$	1.01	523	0.70

Experimental Section

Samples and Solutions. Six poly(styrene-*b*-isoprene) diblock copolymers were synthesized by living anionic polymerization, following standard procedures.[7] Styrene was purified by stirring over calcium hydride, followed by vacuum distillation and treatment with *n*-butyllithium. Isoprene was treated with dibutylmagnesium followed by *n*-butyllithium. The polymerizations were carried out in cyclohexane, which had been distilled from *n*-butyllithium. The initiator was *sec*-butyllithium, and the polymerization of styrene proceeded for 4 h at 40 °C, followed by 4 h for isoprene at the same temperature.

The polymers were characterized by size exclusion chromatography (SEC) with multiangle light scattering detection (Wyatt DAWN) and by ^{1}H NMR. The overall weight-average molecular weight, M_w, and polydispersity, M_w/M_n, were determined for each polymer from the light scattering signal. The samples are designated SI($X-Y$), where X and Y denote the PS and PI block molecular weights in kg/mol. The mole fractions of styrene and isoprene repeat units, and the polyisoprene microstructures, were determined by ^{1}H NMR. In all cases the degree of polymerization and the composition agreed very well with the values calculated on the basis of stoichiometry, assuming complete conversion. The estimated uncertainties are ±5% in M_w and ±0.5% in composition. The PI microstructure corresponds consistently to 94 ± 1% 4,1 addition. The compositions were converted to volume fraction of styrene, f, assuming additivity of volumes and densities of 1.05 and 0.913 g/mL for PS and PI, respectively. The degree of polymerization, N, was calculated in terms of a polystyrene reference segment volume. The sample characteristics are compiled in Table 1.

The solvents di-*n*-butyl phthalate, diethyl phthalate, and dimethyl phthalate were obtained from Aldrich. As dialkyl phthalates can undergo slow hydrolysis, each solvent was rigorously purified prior to use. Washing with 5% aqueous sodium bicarbonate followed by repeated washing with distilled water removed phthalic acid and then residual salts. Any remaining water and alcohols were removed by drying overnight with calcium chloride. The solvents were then vacuum distilled (150 °C and 3 mmHg) and stored in a desiccator prior to use. Solutions were prepared gravimetrically, using methylene chloride as a cosolvent. The cosolvent was removed under a gentle flow of nitrogen, and then mild vacuum, until constant weight was achieved. Concentrations were converted to polymer volume fraction, ϕ, assuming additivity of volumes and densities of 1.043, 1.118, and 1.16 g/mL for DBP, DEP, and DMP, respectively. Solutions were stored in a freezer at −20 °C to inhibit degradation. Additionally, each solution contained 0.1 wt % of polymer of the antioxidant BHT (2,6-di-*tert*-butyl-4-methylphenol). Several control samples were prepared with and without BHT, and as expected there was no discernible effect on the phase behavior. For samples that were exposed to temperatures above 175 °C, SEC was used after the fact to ensure that no degradation had taken place.

Small-Angle X-ray Scattering. SAXS was used to confirm all ordered phase assignments. Measurements were made

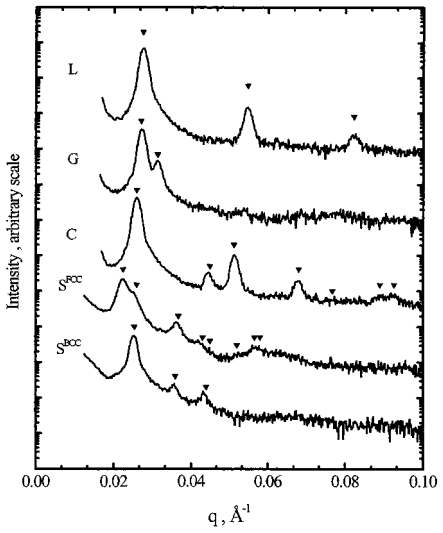

Figure 2. Representative SAXS traces illustrating the five morphologies for SI(15−13) in DEP solutions: lamellar (L) for $\phi = 0.71$ at 65 °C; gyroid (G) for $\phi = 0.66$ at 80 °C; cylinder (C) for $\phi = 0.71$ at 50 °C; S^{fcc} for $\phi = 0.23$ at 50 °C; S^{bcc} for $\phi = 0.23$ at 80 °C. The arrows indicate the relative positions for the first few allowed reflections for each structure.

utilizing Cu Kα X-rays ($\lambda = 1.54$ Å) from a Rigaku RTU-200BVH rotating anode. Franks mirrors were used to focus the beam onto an area detector (Siemens HI-STAR), typically placed about 2 m behind the sample. Sample temperatures were controlled to ±0.2 °C using a thermostated brass block. Two-dimensional images were corrected for detector response, azimuthally averaged, and placed on an intensity vs wavevector ($q = 4\pi \sin(\theta/2)/\lambda$) scale using duck-foot collagen to calibrate the scattering angle. Typical exposure times were 1−20 min at a given temperature. Solutions were sealed under inert atmosphere in 1.5 mm quartz capillaries (Charles Supper Co.). Samples were annealed for at least 5 min at a given temperature prior to measurement, and sometimes for much longer off-line, to ensure structural equilibration. Examples of the scattering patterns are shown in Figure 2 for various solutions of SI(15−13) in DEP; the concentrations and temperatures are chosen to illustrate lamellar, gyroid, hexagonal cylinders, fcc spheres, and bcc sphere phases.

Rheology. Rheological characterization was performed on an ARES instrument (Rheometric Scientific), using parallel plates of 25 or 50 mm diameter and gap widths of 0.5−1 mm. Care was taken to ensure that strain amplitudes were sufficiently small to remain within the regime of linear viscoelastic response. As temperature was controlled via a nitrogen convection oven, possible effects of solvent evaporation and/or sample degradation were checked by repeating high-temperature measurements. (The boiling points of DBP, DEP, and DMP are ca. 340, 299, and 282 °C, respectively.) Measurements of the dynamic moduli G' and G'' were made in two modes: at a fixed low frequency as a function of temperature or as a function of frequency at fixed temperature. The former protocol is well established as an effective means to locate order−order transitions (OOT) and the order−disorder transition (ODT) and was used extensively in this work.[1,7,8,21,22] In these experiments the typical frequency was below 1 rad/s, and the heating rate was 1 °C/min. The second protocol is useful for identifying the morphology, as the low-frequency response of the different phases have characteristic signatures. Figure 3 shows examples of both ODTs and OOTs determined from $G'(T)$, for SI(22−12) in DBP at the indicated concentrations.

Static Birefringence. Static birefringence, or more correctly depolarization of transmitted light, is a simple and convenient means to locate OOTs and ODTs in block copolymer samples.[7,8,23,24] Vertically polarized light from a HeNe laser is directed through the sample and a horizontal analyzing polarizer onto a photodiode. Samples in isotropic states

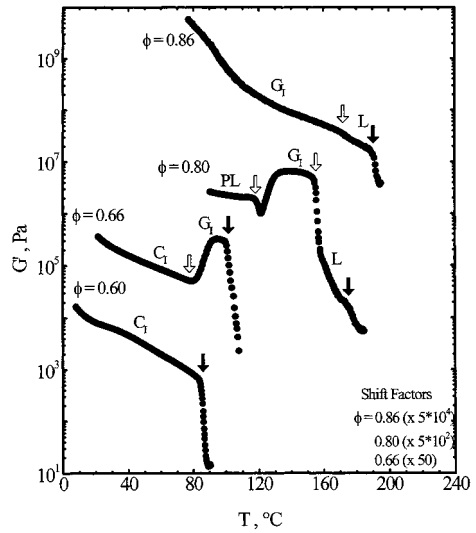

Figure 3. Representative dynamic elastic moduli, G', vs temperature for SI(22−12) in DBP at the indicated concentrations. The curves have been shifted vertically for clarity. Open arrows denote order−order transitions, and filled arrows denote order−disorder transitions.

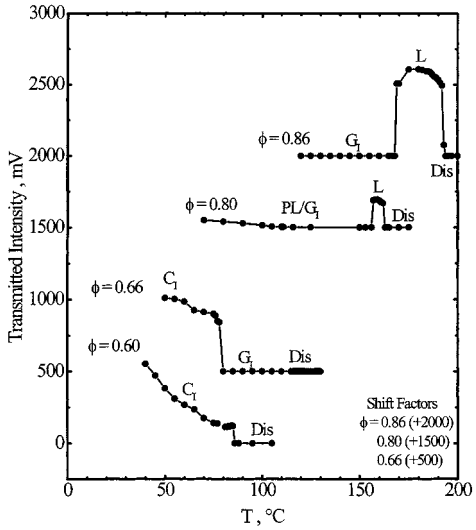

Figure 4. Representative depolarized transmitted intensities vs temperature for the same solutions as in Figure 3. The curves have been shifted vertically for clarity.

(disordered or cubic) do not depolarize the light, and no signal is recorded, whereas lamellar or hexagonal phases are birefringent. In a typical experiment the sample (confined between glass disks and sealed with high-temperature adhesive) is subjected to a slow temperature increase (less than 1 °C/min), and a transition is indicated by the abrupt appearance or disappearance of transmitted intensity. For the systems examined here, only ODTs from cubic phases could not be detected in this manner. Examples of OOTs and ODTs from static birefringence are shown in Figure 4 for the same solutions as in Figure 3. These results exemplify the complementarity of the two techniques. For example, the OOT between G and L for $\phi = 0.86$, and the small window of L for $\phi = 0.80$, would be very difficult to discern on the basis of G' alone (Figure 3) but are prominent features in the birefringence (Figure 4). Conversely, the existence of G between C and DIS for $\phi = 0.66$ is invisible in birefringence but very clear in rheology.

Dynamic Light Scattering. Dynamic light scattering was used to locate the critical micelle temperature (cmt) for each copolymer in each solvent (where accessible) at $\phi \approx 0.01$ and to determine the hydrodynamic radius (R_h) of the micelles as

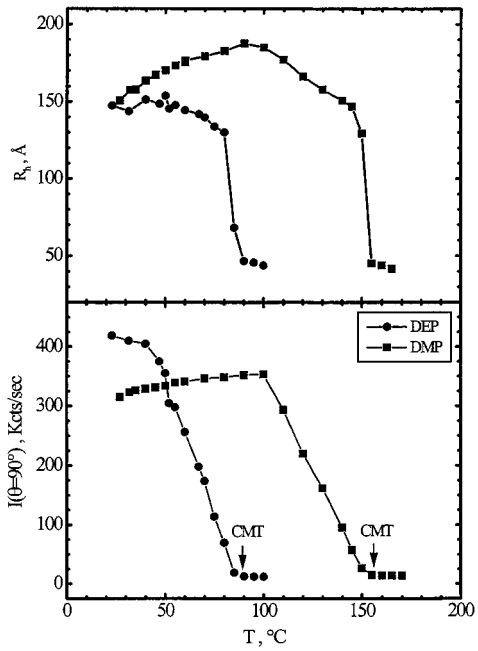

Figure 5. Hydrodyamic radii (upper panel) and scattered intensities at $\theta = 90°$ for SI(15−13) at $\phi = 0.01$ in DEP and DMP. The critical micelle temperatures are indicated by the arrows.

a function of temperature. Measurements were taken on a home-built apparatus using either an argon ion ($\lambda = 488$ nm) or a helium−neon ($\lambda = 633$ nm) laser and a Brookhaven multitau correlator (BI9000). Intensity correlation functions were recorded at three or more scattering angles θ, and fit to single-exponential decays. Representative examples of the resulting data are shown in Figure 5, where R_h and the scattered intensity I (at $\theta = 90°$) are plotted as a function of T of SI(15−13) in DEP and DMP. The cmt is taken as the onset of the first significant departure from the high-T asymptotes in I, following standard practice.[25] Below the cmt both quantities first increase smoothly with decreasing T, and then begin to decrease slightly, about 40−50 deg below the cmt. This interesting decrease presumably reflects a shrinking of the micelles as the solvent becomes more selective.

Results

This section is organized as follows. We begin with some general comments about the details of the experimental results, which are too numerous to present in full.[26] Then we present the phase diagrams (ϕ,T) for four different values of f in the various solvents; the results for a fifth polymer, SI(11−21), have been presented before,[7,8] and a sixth, SI(8−7), is only considered in one solvent. These data are then collected to present representative examples of the other two planes of the phase cube, primarily for DEP. We conclude with more discussion of the results and how they may be understood.

General Comments. All of the transitions reported (ODTs and OOTs) were located by at least two of the three techniques (SAXS, rheology, and birefringence). In all cases the transition temperatures from the different techniques agreed very well, i.e., usually to within 1 or 2 °C and at worst 5 °C. The transitions were routinely located upon heating. The fact that the different techniques agree, even though rather different heating rates were employed, suggests that the transition temperatures are close to the equilibrium values. Care was taken to ensure that all of the transitions were thermally reversible, although the kinetics of OOTs can depend strongly on ϕ, T, and the nature of the transition. Two transitions that are typically quite slow (i.e., sometimes requiring hours or even days) are lamellar to gyroid (L → G) and bcc spheres to fcc spheres ($S^{bcc} \rightarrow S^{fcc}$). However, the experimental situation is not as bleak as it might at first appear. For L → G, the L rapidly transforms to a metastable, intermediate perforated layer (PL) structure, which is readily detected;[7,8,27] the L → PL transition temperature is very close to the equilibrium L → G point.[7,8] The $S^{bcc} \rightarrow S^{fcc}$ transition only occurs for a few solutions in this study and always on cooling; because the reverse transition on heating was rapid, the presence of the transition was signaled in advance. The phase diagrams also indicate a region termed "glass" at large ϕ and low T. This represents an estimate of where the polystyrene domains were near or below the glass transition, such that equilibration was impractical. The experimental signatures of this phenomenon were rather clear, namely the temperature dependence of the primary SAXS peak position, q^*, would change, and the peak width would increase rather than decrease on cooling. It is worth noting another advantage of the dialkyl phthalates in this context; being styrene-selective, they plasticize the styrene domains and thereby minimize the glassy window. In contrast, several previous studies of SI copolymers in isoprene-selective solvents, such as decane, tetradecane, and squalane, were more limited by this phenomenon.[6,9] As an additional practical note, although the dialkyl phthalates do provide a wide temperature window, they can evaporate to a measurable extent. In such cases SAXS and birefringence become the preferred characterization tools because the samples can be sealed.

A brief discussion of nomenclature is appropriate here. We will denote the various states as lamellar (L), cylinder (C), gyroid (G), spheres (S), and disordered (DIS). The S phase will be denoted with a superscript fcc or bcc, and when appropriate the component that forms the minor domain in C, G, or S will be specified by a subscript I or S. Although this nomenclature is quite transparent, and relatively common in the block copolymer literature, it differs from those sometimes employed in the surfactant and lyotropic liquid crystal fields. For example, what we term L, C_I, and C_S would be referred to as L_α, H_I, and H_{II}, respectively, if we take styrene as the "hydrophilic" block.

Phase Diagrams for Particular Polymers. The phase diagrams for the most isoprene-rich diblock, SI(11−32), in DOP, DBP, and DEP are shown in Figure 6a−c, respectively; the behavior in DMP was not determined. The result in the neutral solvent DOP is included here as a reference to illustrate how the increasing selectivity exerts a profound effect on the extent of the ordered phases and on their multiplicity. The full characterization of the neutral solvent case will be presented elsewhere.[14] In these figures and throughout, the solid circles represent experimental ODTs and the open circles OOTs. The smooth curves which "connect the dots" are guides to the eye and are intended to present plausible estimates of the associated phase boundaries. In fact, regions of phase coexistence are anticipated along all of these boundaries, but they are evidently extremely narrow, as the measured transitions were apparently complete over a 2−3 °C interval. This is in accord with previous reports[7,8] and with theoretical expectation.[28] The one exception to this general observation is provided by broad regions of L +

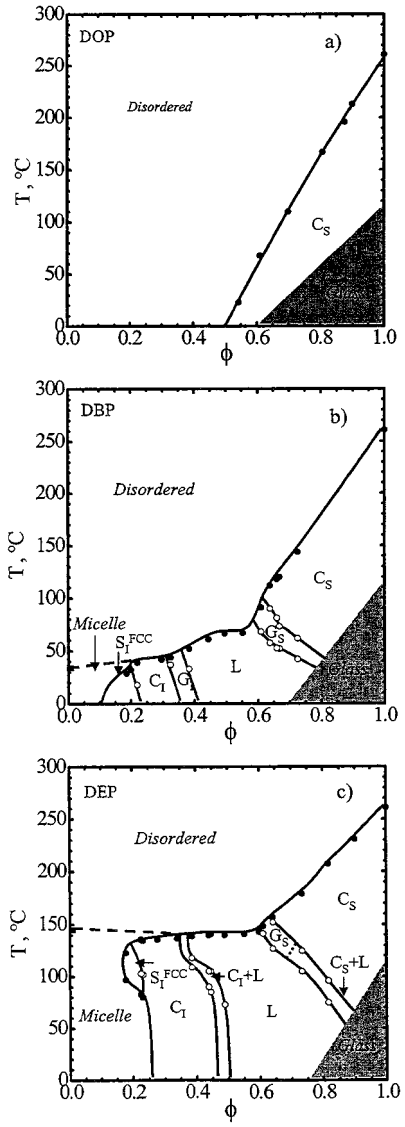

Figure 6. Phase diagrams for SI(11−32) in (a) DOP, (b) DBP, and (c) DEP.

C coexistence, which are seen in certain cases where G might be anticipated. The reason for this will be addressed subsequently. The dashed lines which appear on the left side of some of the phase diagrams connect the dilute solution cmt, determined at $\phi \approx 0.01$, to the ODTs in the nearby ordered states. The connection between these quantities will be discussed further subsequently, but for now it is important to recall that the ODT in this case is always a first-order thermodynamic phase transition, whereas the cmt is not a true phase transition. Thus, the micellar solutions seen at low ϕ and low T in selective solvents are formally part of the disordered phase.

The neutral solvent phase diagram in Figure 6a shows that the addition of solvent rapidly and systematically depresses the ODT, which in this case corresponds to $C_S \rightarrow$ DIS. As the solvent is distributed essentially uniformly, there is no change to the spontaneous curvature of the styrene/isoprene interface, and thus no OOTs are induced. The rate at which the ODT is lowered is significantly greater than that anticipated by the so-called "dilution approximation", whereby the phase behavior is predicted to be governed solely by an effective interaction parameter given by $\phi\chi$.[29−32] This non-mean-field result has been extensively documented for lamellar and asymmetric diblocks[7,8,12,14] and is broadly attributable to an additional stabilization of the disordered phase arising from polymer/solvent as well as polymer/polymer fluctuations. Moving to Figure 6b, the introduction of a modest selectivity exerts a strong influence on the phase diagram; at low temperature the sequence of phases upon dilution is $C_S \rightarrow G_S \rightarrow L \rightarrow G_I \rightarrow C_I \rightarrow S_I^{fcc}$. The interesting observation that the S_I packing is fcc may be attributed to the copolymer composition. In this case, the shorter styrene blocks form the micellar corona, and thus the micelle is "crew-cut"; the resulting short-range, hard-sphere-like potential favors the fcc packing.[6,33] All of the boundaries between ordered phases tilt to the left. This is a direct result of the temperature dependence of the selectivity; i.e., as T increases, DBP becomes less selective. Consequently, the solvent partitions extensively into the styrene domains at low T but then begins to redistribute itself more uniformly upon heating. Thus, the thermotropic OOTs all reflect what would be expected if one were to decrease the styrene fraction, f.

As the selectivity is increased, to DEP, the same trends are followed, but the ODT temperatures are increased significantly. In this instance the aforementioned C + L coexistence is observed for both C_S + L and C_I + L. It should be noted that this coexistence is the equilibrium state, because it could be accessed both by heating and by cooling, because the X-ray peak intensities associated with the two phases followed a lever rule as T was varied across the coexistence window, and because the state was stable upon prolonged annealing (>1 month). As proposed previously,[8] we attribute the coexistence to the packing frustration inherent in the gyroid structure, which in the melt is believed to truncate the window of G as the degree of segregation (χN) is increased.[34,35] In other words, at very low temperature a bulk copolymer in G should transform to either L or C. In solution, however, the additional degree of freedom allows the system to lower its free energy by escaping G at a lower effective degree of segregation. An additional interesting feature in Figure 6c is the "cusplike" nature of the S^{fcc} window and the reentrant ODT that is observed near $\phi \approx 0.2$. This feature is presumably a result of solvent swelling of the micelle cores as T increases and the solvent becomes less selective. A congested solution of micelles could be just on the brink of the ordering transition, by analogy to hard spheres at a volume fraction near 0.49, and a small expansion of the micellar size drives the ordering process.

The phase behavior for the next polymer in the sequence of increasing f, SI(11−21), has been described previously[7,8] and so is not presented here. Accordingly, we now turn to SI(15−13), a nearly symmetric copolymer that therefore forms L in the bulk. The phase diagrams in DBP, DEP, and DMP are shown in Figure 7a−c, respectively. In all three solvents the sequence L $\rightarrow G_I \rightarrow C_I \rightarrow S_I$ is observed with dilution at low temperature, with the ODT temperatures at fixed ϕ increasing steadily with increasing solvent selectivity. The remarkable new feature here is the presence of both bcc and fcc phases and the reversible, thermotropic transitions between them in DEP and DMP. This aspect of the phase behavior has been considered in more detail elsewhere,[26,36,37] but a few comments are in order. The transition is epitaxial, and the number of micelles is

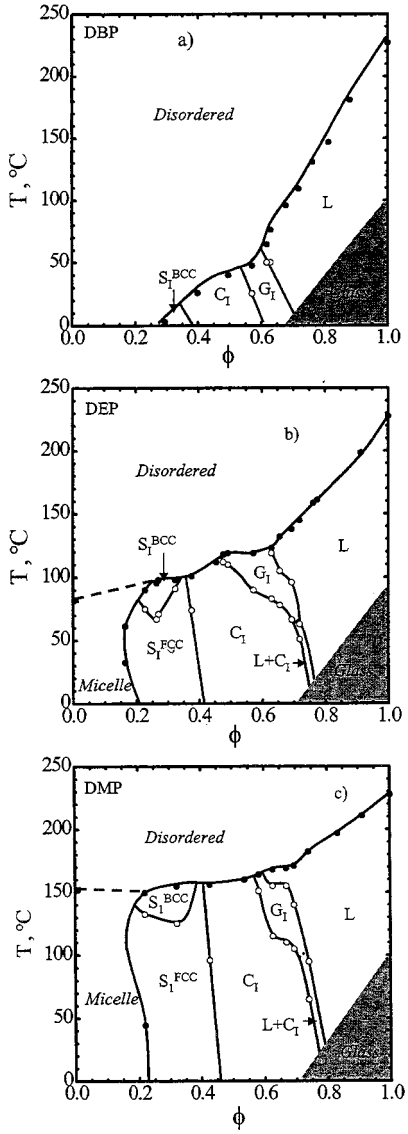

Figure 7. Phase diagrams for SI(15−13) in (a) DBP, (b) DEP, and (c) DMP.

conserved.[36,37] The transition appears to be driven by micellar core swelling, just as is the reentrant ODT. The bcc structure has slightly closer nearest neighbors, but fewer of them (8 vs 12 for fcc), and apparently is favored as the micelles become bigger (and, possibly, softer in terms of the intermicellar potential). It is interesting to note that the transition occurs when the ratio of the corona thickness, L_c, to the core radius, R_c, is about 0.5, which is very far from the fcc/bcc boundary proposed by McConnell and Gast for SI copolymers in decane ($L_c/R_c \approx 1.5$).[6,33] This thermotropic transition is also different from that seen by Hamley and co-workers for PEO−PBO micelles in water.[38,39] In that case the decreasing solvent quality of water for the PEO corona with increasing T drives a shrinking of the corona block and thus a transition from "hairy", bcc-forming micelles to "crew-cut", fcc-forming ones. In the current system, the solvated PS block is in good solvent conditions at all temperatures considered, and the relatively subtle changes in micellar dimensions are primarily due to solvent entering the core.

To assess whether this interesting behavior is dependent on molecular weight, we examined the phase behavior of SI(8−7) in DMP, a polymer of comparable

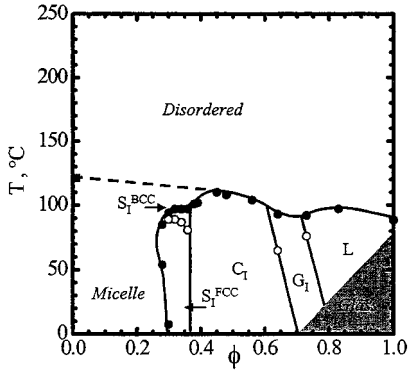

Figure 8. Phase diagrams for SI(8−7) in DMP.

composition to SI(15−13). The results are shown in Figure 8. Clearly the $S^{fcc} \rightarrow S^{bcc}$ transition persists, and indeed the phase behavior overall is quite comparable to that in Figure 7c. The disordered micellar solution persists to higher concentrations, $\phi \approx 0.3$, presumably due to a smaller micellar radius and therefore smaller effective volume fraction of spheres. Figure 8 also illustrates another important point, namely that the melt ODT is determined through styrene/isoprene interactions, i.e., by χN, whereas the dilute solution cmt is determined by isoprene/solvent interactions. Consequently, when N was halved in going from SI(15−13) to SI(8−7), the melt ODT dropped from ca. 230 to 90 °C, whereas the cmt only fell from ca. 150 to 120 °C. As a result, the ODT temperature is roughly independent of ϕ in Figure 8. Clearly, also, for a sufficiently selective solvent the ODT temperature can be made to *increase* upon addition of solvent, an effect which is well-known in nonionic surfactant/water solutions and which has recently been demonstrated for SI diblocks in isoprene-selective solvents.[9]

Figures 9a−c and 10a−c show the phase behavior in DBP, DEP, and DMP for SI(22−12) and SI(38−14), respectively. In these cases the trends are rather easily understood. For SI(22−12), the melt sample lies just within the L window and quickly progresses to G_I, followed by C_I and S_I with added solvent. The metastable PL window is noted by a dashed line, as the proximity to the glass transition inhibited the kinetics of the PL → G, and thus this latter transition was not confirmed. In all cases the observed S phase was bcc, consistent with the "hairy micelle" argument, although the L_c/R_c ratios were typically about 1.2, again quantitatively inconsistent with the criterion suggested by McConnell and Gast.[6,33]

(*ϕ*,*f*) and (*T*,*f*) Slices through the Phase Cube. The isothermal phase behavior of SI copolymers in DEP as a function of composition and concentration is presented in Figure 11a−d for T = 200, 150, 100, and 50 °C, respectively. In these diagrams the dashed lines correspond to phase transitions that are presumed to exist but were not actually encompassed by the samples employed. At the highest T, the solvent is almost neutral, and accordingly the diagram is almost symmetric about $f = 0.5$ as it would be in the melt. The protrusion of the phase boundaries to lower ϕ for the C_S and C_I samples is not significant; it simply reflects the differing values of N for the various polymers. Upon cooling to 150 °C, the area of ordered phases increases, and the phase boundaries begin to shift to the left. This is indicative of the onset of solvent selectivity; DEP begins to swell the PS domains preferentially, and

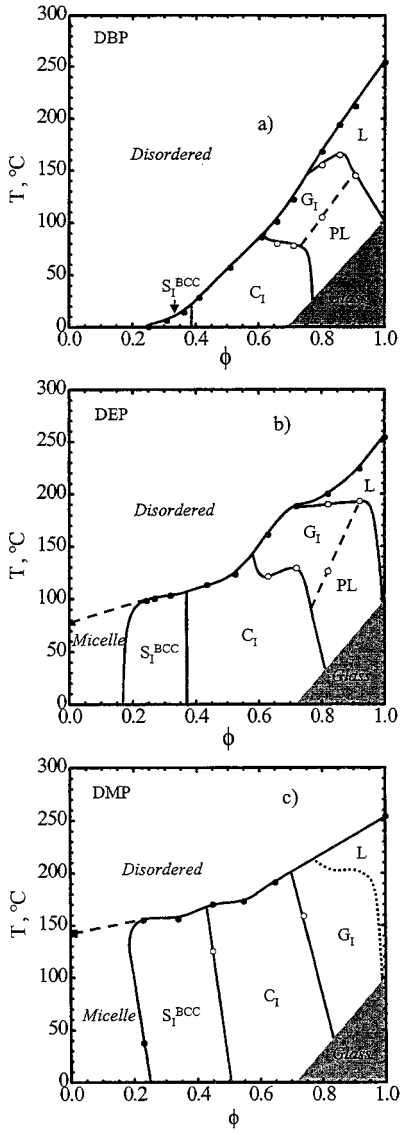

Figure 9. Phase diagrams for SI(22−12) in (a) DBP, (b) DEP, and (c) DMP.

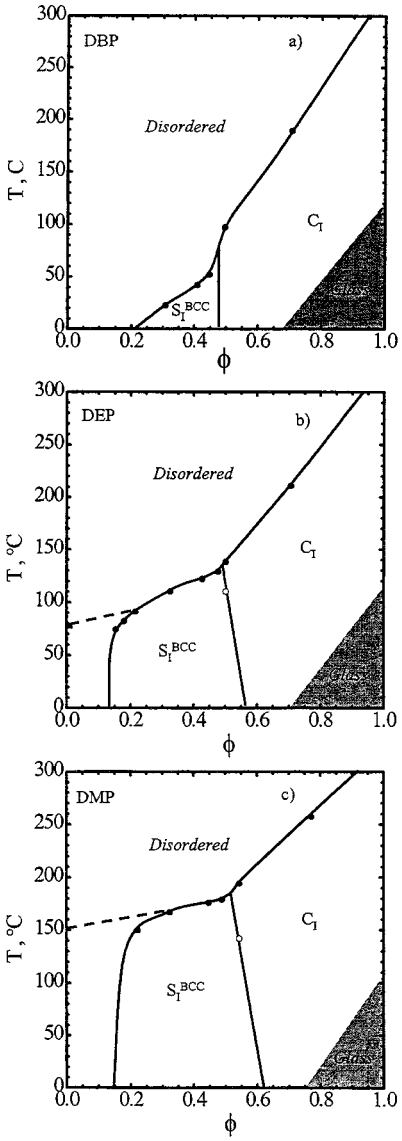

Figure 10. Phase diagrams for SI(38−14) in (a) DBP, (b) DEP, and (c) DMP.

therefore the effective fraction of styrene (i.e., f + solvent) increases. At the same time, the OOT boundaries begin to tilt to the left, for the same reason: as more solvent is added, the tendency for the interfaces to curve toward the PI domains increases. In Figure 11c, corresponding to 100 °C, these various effects are greatly magnified. The L + C coexistence windows become apparent, and the separate fcc and bcc phases appear as a function of f. By 50 °C, shown in Figure 11d, the glassy region begins to intervene, thereby obscuring a series of OOT lines emanating from the L/G, G/C, and C/S boundaries on the melt ($\phi = 1$) axis. At 50 °C, also, there is a clear fcc/bcc boundary, falling in the range $0.5 < f < 0.6$. The disordered phase associated with the lyotropic ODT in Figure 11d is a micellar solution for almost all compositions. Not indicated on this plot are regions of macrophase separation, anticipated in the limit $f \rightarrow 0$, and a line of cmcs in the limit $\phi \rightarrow 0$. The micelles must also vanish in the limit $f \rightarrow 1$ for all ϕ. Figure 11d implies (as do Figures 12c and 13e) that there are ODTs from C and L into micellar solutions. This, in turn, suggests that the resulting micelles might be anisotropic in shape. This interesting point is beyond the scope of the present paper, but we note that highly asymmetric (isoprene-rich) SI copolymers in DBP were previously reported to produce ellipsoidal micelles close to the C/micelle boundary.[4,5,40]

The corresponding slices through the phase cube for DBP solutions are shown in Figure 12a−c for 100, 50, and 0 °C, respectively. In this case the solvent is nearly neutral at 100 °C, and so there is relatively little asymmetry in the diagram and relatively little tilting of the OOT lines. Indeed, this plot is very similar to that for DEP at 150 °C (Figure 11b), underscoring how these solvents exhibit a steady progression in selectivity. Similarly, at 0 °C in DBP (Figure 12c) the behavior is rather like DEP at 50 °C (Figure 11d). However, two important differences are the reduction in the fcc window relative to bcc, with this transition now falling in the range $0.2 < f < 0.3$, and the boundary between micellar and nonmicellar disordered solutions (dashed line). Both of these features are attributable to the temperature dependence of the solvent/isoprene interactions. Only for rather small f do micelles form at this temperature, and only for small f is the segregation strong enough to form crew-cut micelles that order on an fcc lattice. From the difference between the values of f at the fcc/bcc boundary in DBP and DEP and from

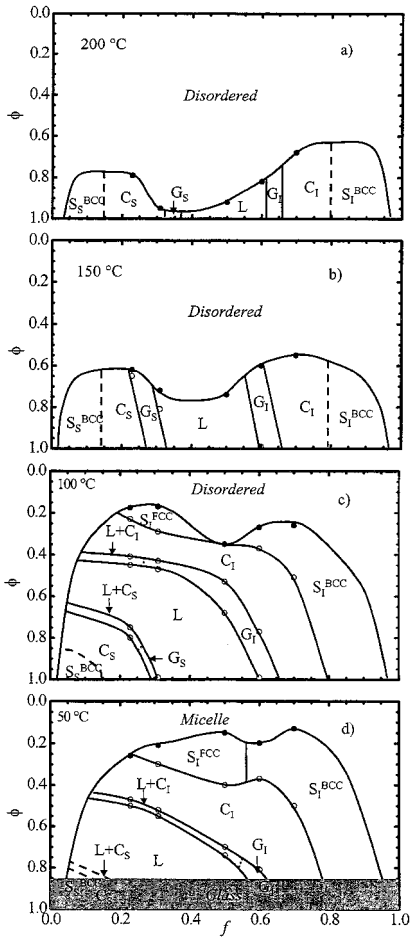

Figure 11. Concentration vs composition maps for SI copolymers in DEP at (a) 200, (b) 150, (c) 100, and (d) 50 °C.

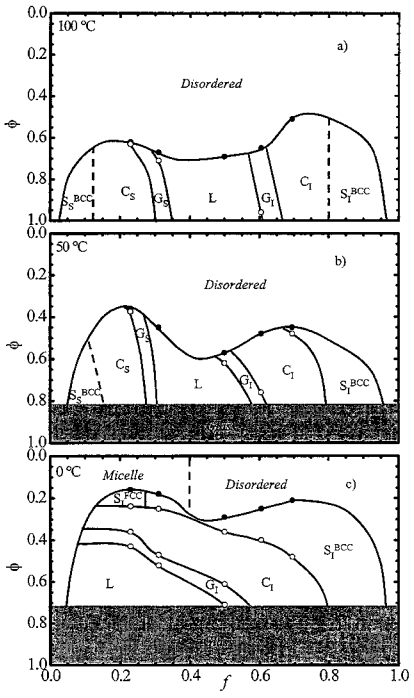

Figure 12. Concentration vs composition maps for SI copolymers in DBP at (a) 100, (b) 50, and (c) 0 °C.

the presence of thermotropic fcc/bcc transitions, we may conclude that there is no simple L_c/R_c criterion for this transition.

The third possible slice through the phase cube, i.e., (T,f) at constant ϕ, is illustrated for DEP at $\phi = 0.9$, 0.7, 0.5, 0.3, and 0.2 in Figure 13a−e, respectively. The progression in behavior follows from the previous perspective. For example, in Figure 13a the modest amount of solvent exerts rather little influence on the melt phase map. There is a slight tilt to the right of the OOT lines, reflecting the low-temperature preferential swelling of the styrene domains and therefore an increase in the scope of the phases with isoprene in the minor domains. As noted before, the corrugation of the line of ODTs is simply an effect of variable total N. Also, the dashed lines demarking the bcc phases are presumed, rather than experimentally established, and they too might tilt to the right. By $\phi = 0.7$ (Figure 13b) the solvent selectivity is much more apparent. The OOT lines have moved significantly to lower f, and the C_I and S_I phases are much more prominent. At $\phi = 0.5$, the C_S and S_S phases have been completely eliminated, and the observed ODT temperatures are almost constant near 120−130 °C. The reason for this "flattening" of the ODT curve, relative to $\phi = 0.9$, is the fact that the ODT is now a reflection of the isoprene/DEP interactions rather than the styrene/isoprene interactions and as such is less sensitive to N. For $\phi = 0.3$ (Figure 13d) only C_I, S_I^{bcc}, and S_I^{fcc} phases are seen, and by $\phi = 0.2$ (Figure 13e) the C_I is almost eliminated. In this slice of the phase cube there is now a wide range of f over which reentrant ODTs are found and also a wide range of f for which the upper ODT is $S^{fcc} \rightarrow$ DIS.

Discussion

The preceding results illustrate the "topology" of the full phase cube of Figure 1 via three orthogonal planes: (ϕ,T) at fixed f, (ϕ,f) at fixed T, and (f,T) at fixed ϕ. The broad features of this behavior may be understood through the concept of trajectories across the melt phase map, described in more detail in a previous report.[8] The essence of this approach is to view the partitioning of the solvent between the two microdomains as equivalent to a variation of f in the melt. This basic idea was proposed years ago by Sadron and Gallot,[2] based on the prior suggestion of Molau that adding A homopolymer to an AB melt was equivalent to increasing f_A.[41] Sadron and Gallot were able to demonstrate how this concept anticipates the observed sequence of phases encountered by adding a selective solvent to a given copolymer, although in these early studies the G phase had not yet been identified.[2] If one begins with an ordered copolymer of small f_A, such that it forms S_A in the bulk, a sequence of lyotropic transitions $S_A \rightarrow C_A \rightarrow G_A \rightarrow L \rightarrow G_B \rightarrow C_B \rightarrow S_B$ should be anticipated with increasing dilution. This would correspond to a horizontal trajectory across the melt phase map, i.e., parallel to the f_A axis. The sequence may be truncated at either end, for example by starting with a copolymer in C_A (Figure 6) or L (Figures 7, 8, or 9) or by the ordered phases giving way to a suspension of micelles before S_B is accessed (low temperatures in Figure 6). This approach is broadly consistent with the results in DBP, DEP, and DMP at lower temperatures, where the solvents are most selective. However, more detailed analysis reveals that the trajectories are not, in fact, horizontal, as the interfacial tension between PI and (PS + solvent) is not independent of ϕ. In fact, at room temperature the addition of DEP and DMP increases the effective segregation between the two microdomains, whereas DBP lessens

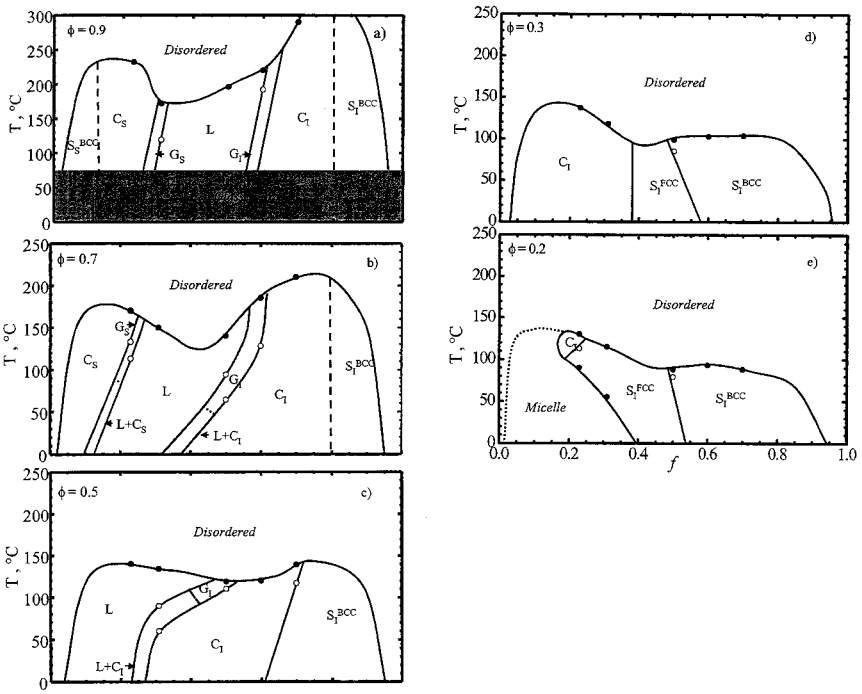

Figure 13. Temperature vs composition maps for SI copolymers in DEP at concentrations of (a) 1, (b) 0.7, (c) 0.5, (d) 0.3, and (d) 0.2.

it to some extent. In other words, PI "prefers" PS relative to DEP and DMP.

The more interesting aspects of the phase behavior occur when temperature is increased at fixed f and ϕ. The boundaries between the various phases in the (ϕ,T) plane tend to "lean" to the left (see Figures 6−10). This is a direct result of the solvent becoming less selective as T increases and consequently partitioning back into the PI microdomain, thereby decreasing the effective f.[8] This effect is captured, at least qualitatively, by self-consistent mean-field theory.[8,32] In the trajectory picture, this would amount to a diagonal trajectory across the phase map with increasing temperature, corresponding to a concurrent reduction in both the effective f and the effective degree of segregation (χN).[8] These results underscore that the addition of selective solvent is qualitatively different from the addition of homopolymer.[42] First, to a good approximation the addition of homopolymer at fixed temperature does not modify the degree of segregation and therefore amounts to a horizontal trajectory across the melt phase map. Second, increasing temperature does not lessen the partitioning of homopolymer into the corresponding microdomain, and so the resulting trajectory is essentially vertical.

As noted in the previous section, there are several features of the various phase diagrams that simply cannot be anticipated on the basis of knowledge of the melt behavior. The two principal examples are the replacement of G by broad regions of L + C coexistence and the existence of both bcc and fcc micellar packings for $\phi \approx 0.2-0.4$. The former is attributed to packing frustration, which Matsen has proposed accounts for the truncation of the G phase at high χN in the melt.[34] Namely, in G there is differential chain stretching between those minor blocks in the center of a "strut" and those that must reach the center of the three-way connection. As the mean stretching increases with segregation, this differential becomes relatively more costly. We hypothesize that the additional degree of freedom in solution allows the system to lower its free energy by separating from G into L + C, at segregations significantly lower than where G is predicted to become unstable in the melt. The bcc/fcc selection is more complicated and will be analyzed in more detail in a subsequent report.[37] We can identify three broad regimes of behavior. For small f, i.e., SI(11−21) and SI(11−32), fcc is more prevalent, whereas for large f, i.e., SI(22−12) and SI(38−14), bcc is observed. This is qualitatively consistent with the McConnell and Gast scenario, namely that "crew-cut" micelles prefer fcc and "hairy" micelles prefer bcc.[6,33] The intermediate regime, with approximately symmetric copolymers, gives rise to the thermotropic transition between fcc and bcc on heating. This transition is reminiscent of many elemental systems[36,43] and can be viewed as an example of the Alexander and McTague conjecture[44] that all spherical objects with weakly first-order melting transitions adopt the bcc packing near the melting line (the ODT in this case), for generic entropic reasons.

The results presented here are sufficient to outline a broad strategy for estimating the phase behavior of a given block copolymer in a given solvent. The two crucial pieces of information are the melt ODT of the copolymer and the cmt of a dilute solution. The former depends on f and χN and the latter primarily on χ_{BS} between the solvent (S) and the unfavored block (B). In particular, the cmt lies some tens of degrees below the Θ temperature ($\chi_{BS} > 0.5$), because it is easier to dissolve an AB copolymer than a B homopolymer, but the cmt will increase as f decreases. For example, the cmt is 145 °C for SI(11−32) in DEP but falls to about 78 °C for SI(38−14); we estimate the Θ temperature to be above 160 °C. Given the melt ODT and the cmt, a line of ODTs connects smoothly to a line of cmts, providing the boundary between dispersed chains at high temperature and either micelles or ordered phases at low temperature. In all cases considered here the boundary between ordered phases and micelles occurs near $\phi \approx 0.2$, but this will depend on N. For larger N, the micelles will be larger and thus pack on a lattice at lower ϕ. We

reiterate that the micellar solution is formally part of the disordered phase and that the boundary between micelles and lattice corresponds to the ODT. Thus, there is no terminus to the line of ODTs, but rather a sharp downturn at some $\phi \approx 0.2$. Given the ODT and cmt, the rest of the phase diagram can be filled in by consideration of the solvent selectivity. At very low temperatures, far below the cmt, the solvent will be completely selective, and the phase boundaries should be vertical. The location of each boundary can be estimated on the basis of the corresponding transition on the melt phase map, assuming that the effective f is given by $f\phi + (1 - \phi)$. With increasing temperature, these boundaries begin to curve to lower ϕ, due to the decreasing solvent selectivity.

The final issue to consider is a brief comparison between these results and those of Lai et al.[9] and McConnell and Gast.[6] For AB diblocks, it should not matter whether one employs A or B selective solvents; the full phase cube should have the same appearance when reflected through the $(T,f = 0.5)$ plane. Thus, our results should be very similar to these other studies. The broad features of the results of Lai et al.[9] in tetradecane are consistent with those presented here. They did not observe the systematic curvature of the phase boundaries that we report, presumably because the selectivity of tetradecane does not change much with temperature. Their results did not extend to dilute solution, and so the cmts were not reported. They also did not observe fcc phases, but their measurements did not emphasize the lower concentrations for smaller values of f. We have, in fact, observed fcc phases and fcc/bcc transitions in squalane, as will be discussed elsewhere.[37] Our results, and those of Lai et al.,[9] do conflict with those of McConnell and Gast[6] in the following respect. As the latter authors increased ϕ in decane solutions, they observed a reentrant order−disorder transition into a disordered phase from S,[6] rather than the S/C boundary that we and Lai et al.[9] find. This remarkable observation was explained on the basis of a star polymer model, whereby the overlapping coronas screened the micelle−micelle repulsion.[6,45] Lai et al. suggest,[9] and we concur, that the solutions of McConnell and Gast were not, in fact, at equilibrium. The decane samples were prepared by solvent evaporation, and the temperature was never raised above 40 or 50 °C.[6] Consequently, at some rather modest ϕ the PS cores become glassy; in effect, the micelles became kinetically cross-linked and behaved like stars. We have confirmed this contention by preparing decane solutions of an SI(15−15) following the McConnell−Gast protocol. A solution with $\phi \approx 0.6$ thus prepared gave rather broad scattering features, quite similar to those reported by McConnell and Gast.[6] However, by heating to 120 °C and cooling, the resulting scattering pattern transformed into a clear hexagonal phase, as would be expected on the basis of Figure 7c.

Summary

The full phase cube (composition, concentration, and temperature) has been explored for SI diblock copolymers in three solvents of differing selectivity toward styrene. The principal conclusions may be summarized as follows.

1. SAXS, rheology, and static birefringence provide a clear and consistent identification of all equilibrium ODTs and OOTs.

2. As the solvent selectivity increases, the cmt for a given copolymer in dilute solution increases, and it also increases with increasing isoprene content for a given solvent.

3. The dilute solution cmt and the melt ODT fix the limits of the boundary between single chain solutions at high T and either ordered phases ($\phi > 0.2$) or micellar solutions ($\phi < 0.2$) at low T.

4. Each solvent becomes less selective as T increases, leading to curved phase boundaries in the (T,ϕ) plane and a rich variety of thermally accessible OOTs.

5. The sequence of phases in the phase cube can be broadly understood in terms of the melt phase map, combined with an understanding of how solvent partitioning between the two microdomains affects the spontaneous interfacial curvature.

6. Several features of the results cannot be anticipated on the basis of the melt results. These include broad regions of lamellae/cylinder coexistence, fcc packings of the spherical micelles, thermoreversible fcc/bcc transitions, and reentrant ODTs for micellar solutions. Qualitative explanations for these various phenomena have been proposed.

7. The results are apparently consistent with other studies of SI copolymer solutions in the literature but inconsistent with others. In particular, the proposal that there is a lyotropic reentrant order−disorder transition[6,45] for polymer volume fractions of order 0.5 is suggested to be an artifact of insufficiently equilibrated solutions.

Acknowledgment. This work was supported by the National Science Foundation, through Awards DMR-9528481 and DMR-9901087, and through the University of Minnesota MRSEC (DMR-9809364). A University of Minnesota Doctoral Dissertation Fellowship awarded to K.J.H. is also appreciated.

References and Notes

(1) Hamley, I. W. *The Physics of Block Copolymers*; Oxford University Press: Oxford, 1998.
(2) Sadron, C.; Gallot, B. *Makromol. Chem.* **1973**, *164*, 301.
(3) Shibayama, M.; Hashimoto, T.; Kawai, H. *Macromolecules* **1983**, *16*, 16.
(4) Lodge, T. P.; Xu, X.; Ryu, C. Y.; Hamley, I. W.; Fairclough, J. P. A.; Ryan, A. J.; Pedersen, J. S. *Macromolecules* **1996**, *29*, 5955.
(5) Hamley, I. W.; Fairclough, J. P. A.; Ryan, A. J.; Ryu, C. Y.; Lodge, T. P.; Gleeson, A. J.; Pedersen, J. S. *Macromolecules* **1998**, *31*, 1188.
(6) McConnell, G. A.; Gast, A. P. *Macromolecules* **1997**, *30*, 435.
(7) Hanley, K. J.; Lodge, T. P. *J. Polym. Sci., Polym. Phys. Ed.* **1998**, *36*, 3101.
(8) Hanley, K. J.; Lodge, T. P.; Huang, C.-I. *Macromolecules* **2000**, *33*, 5918.
(9) Lai, C.; Russel, W. B.; Register, R. A. *Macromolecules* **2002**, *35*, 841.
(10) Seddon, J. M. *Biochim. Biophys. Acta* **1990**, *1031*, 1.
(11) Hajduk, D. A.; Kossuth, M. B.; Hillmyer, M. A.; Bates, F. S. *J. Phys. Chem. B* **1998**, *102*, 4269.
(12) Lodge, T. P.; Pan, C.; Jin, X.; Liu, Z.; Zhao, J.; Maurer, W. W.; Bates, F. S. *J. Polym. Sci., Polym. Phys. Ed.* **1995**, *33*, 2289.
(13) Lodge, T. P.; Hamersky, M. W.; Hanley, K. J.; Huang, C.-I. *Macromolecules* **1997**, *30*, 6139.
(14) Lodge, T. P.; Hanley, K. J.; Alahapperuma, V. Manuscript in preparation.
(15) Wanka, G.; Hoffmann, H.; Ulbricht, W. *Macromolecules* **1994**, *27*, 4145.
(16) Zhou, Z.; Chu, B. *Macromolecules* **1994**, *27*, 2025.
(17) Mortensen, K.; Brown, W.; Jorgenson, E. *Macromolecules* **1994**, *27*, 5654.
(18) Mortensen, K. *J. Phys.: Condens. Matter* **1996**, *8A*, 103A.

(19) Pople, J. A.; Hamley, I. W.; Fairclough, J. P. A.; Ryan, A. J.; Komanschek, B. U.; Gleeson, A. J.; Yu, G.-E.; Booth, C. *Macromolecules* **1997**, *30*, 5721.
(20) Svensson, M.; Alexandridis, P.; Linse, P. *Macromolecules* **1999**, *32*, 637.
(21) Bates, F. S.; Fredrickson, G. H. *Annu. Rev. Phys. Chem.* **1990**, *41*, 525.
(22) Fredrickson, G. H.; Bates, F. S. *Annu. Rev. Mater. Sci.* **1996**, *26*, 503.
(23) Balsara, N. P.; Perahia, D.; Safinya, C. R.; Tirrell, M.; Lodge, T. P. *Macromolecules* **1992**, *25*, 3896.
(24) Balsara, N. P.; Garetz, B. A.; Dai, H. J. *Macromolecules* **1992**, *25*, 6072.
(25) Tuzar, Z.; Kratochvil, P. In *Surface and Colloid Science*; Matijevic, E., Ed.; Plenum Press: New York, 1993; Vol. 15.
(26) Hanley, K. J. Block Copolymers: Phase Behavior in Neutral and Selective Solvents. Ph.D. Thesis, University of Minnesota, 2001.
(27) Hajduk, D. A.; Takenouchi, H.; Hillmyer, M. A.; Bates, F. S.; Vigild, M. E.; Almdal, K. *Macromolecules* **1997**, *30*, 3788.
(28) Fredrickson, G. H.; Leibler, L. *Macromolecules* **1989**, *22*, 1238.
(29) Helfand, E.; Tagami, Y. *J. Chem. Phys.* **1972**, *56*, 3592.
(30) Hong, K. M.; Noolandi, J. *Macromolecules* **1983**, *16*, 1083.
(31) Banaszak, M.; Whitmore, M. D. *Macromolecules* **1992**, *25*, 3406.
(32) Huang, C.-I.; Lodge, T. P. *Macromolecules* **1998**, *31*, 3556.
(33) McConnell, G. A.; Gast, A. P.; Huang, J. S.; Smith, S. D. *Phys. Rev. Lett.* **1993**, *71*, 2102.
(34) Matsen, M. W.; Bates, F. S. *Macromolecules* **1996**, *29*, 1091.
(35) Matsen, M. W.; Bates, F. S. *J. Chem. Phys.* **1997**, *106*, 2436.
(36) Lodge, T. P.; Bang, J.; Wang, X. *Phys. Rev. Lett.*, submitted.
(37) Bang, J.; Lodge, T. P. Manuscript in preparation.
(38) Hamley, I. W.; Pople, J. A.; Diat, O. *Colloid Polym. Sci.* **1998**, *276*, 446.
(39) Hamley, I. W.; Daniel, C.; Mingvanish, W.; Mai, S.-M.; Booth, C.; Messe, L.; Ryan, A. J. *Langmuir* **2000**, *16*, 2508.
(40) Pedersen, J. S.; Hamley, I. W.; Ryu, C. Y.; Lodge, T. P. *Macromolecules* **2000**, *33*, 542.
(41) Molau, G. E. *Block Polymers*; Plenum: New York, 1970.
(42) Winey, K. I.; Thomas, E. L.; Fetters, L. J. *Macromolecules* **1992**, *25*, 2645.
(43) Donohue, J. *The Structures of the Elements*; Wiley: New York, 1974.
(44) Alexander, S.; McTague, J. *Phys. Rev. Lett.* **1978**, *41*, 702.
(45) McConnell, G. A.; Gast, A. P. *Phys. Rev. E* **1996**, *54*, 5447.

MA0200975